Paper No. 1705. (quote when citing this article)
Eleventh World Conference on Earthquake Engineering
ISBN: 0 08 042822 3

SEISMIC CRACKING ANALYSIS OF PINE FLAT DAM: CASE STUDY

V. BATTA[1] and O. A. PEKAU[2]

[1]SNC-Lavalin Inc., Montreal, Canada H3B 4P3
[2] Department of Civil Engineering, Concordia University, Montreal, Canada H3G 1M8

ABSTRACT

Seismic cracking behavior of the Pine Flat dam is investigated using the two-dimensional boundary element procedure developed previously. Linear elastic fracture mechanics is employed to monitor crack growth in a multiple, discrete crack propagation analysis of the dam. The predicted fracture response comprises complete rupture of the dam near the base of the crest block. A parametric study of the effect of increasing the magnitude of concrete fracture toughness indicates that, with higher concrete toughness, cracking will also involve other regions of the dam in addition to that occurring near the base of the crest block.

KEYWORDS

Pine Flat dam; seismic cracking; LEFM; boundary elements; discrete cracks.

INTRODUCTION

Seismic cracking behavior of concrete gravity dams has been investigated in a number of studies employing both finite element (Ayari and Saouma, 1990; Bhattacharjee and Léger, 1993) and the boundary element (Pekau *et al.* 1991; Pekau and Batta, 1994) methods. Most of these studies have utilized the classical example of the Koyna dam as the application problem, which facilitates validation of analytical results through comparison with the observed cracking. Since this dam has a non-typical cross-section arising out of the unusually large crest block, it is not apparent that the observations made on the seismic cracking of the Koyna dam are applicable to typical gravity dams. Studies employing typical gravity dams, on the other hand, were based on procedures in which certain analytical factors influenced the results.

The present paper investigates the seismic cracking of the Pine Flat dam which represents a typical gravity-type concrete dam. The dam is located in Kern County, California, and is susceptible to strong earthquake ground motions, making it suitable for a case study of seismic fracture behavior. The dam has been analyzed previously for earthquake induced cracking by Chapuis *et al.* (1985), who employed the finite element method and a hybrid smeared-discrete cracking model incorporating the principles of linear elastic fracture mechanics (LEFM). The main cracking was shown to originate on the upstream face near the crest, but crack propagation could not be monitored completely due to the geometric constraints imposed by the coarseness of the finite element mesh. Seismic analysis of the dam by El-Aidi and Hall (1991a; 1991b) featured the

investigation of the fracture behavior along pre-determined planes of weakness using the smeared crack technique in a finite element mesh. The size of the mesh was, however, found to influence the results in this case also. Detailed cracking analysis of the dam has also been reported by Vargas-Loli and Fenves (1989), who adopted smeared crack modelling together with the crack band theory to conserve the fracture energy. However, due to limitation on the size of the finite elements the concrete fracture energy could not be conserved at a realistic level, which led to a very diffused pattern of the computed cracking.

In the following, earthquake-induced cracking in the Pine Flat dam is investigated employing the boundary element method and discrete crack propagation analysis procedure presented earlier by the authors (Pekau and Batta, 1992). Results for the fracture response of the dam are presented, together with a parametric examination of the influence on the predicted cracking of the magnitude of the dynamic fracture toughness of the concrete .

REVIEW OF ANALYTICAL PROCEDURE

In the boundary element procedure employed herein, the dynamic problem is formulated in the time domain using the frequency independent fundamental solution corresponding to an infinite domain. Discrete crack modelling is adopted for fracture simulation and the multidomain approach is utilized, wherein the cracked dam is divided into subdomains using the existing crack profiles up to the crack tip and introducing arbitrary lines from each crack tip to the opposite boundary. Independent boundary integral expressions for these subdomains are formulated and combined, employing continuity and equilibrium conditions over the common (i.e. connected) portions of the subdomains. Discretization of the boundary of the dam, by means of isoparametric elements, is used to transform the governing equations to matrix form. In front of the crack tips special traction singular quarter-point elements are introduced to represent the required stress singularity.

The equations of dynamic equilibrium are solved by direct integration using the Houbolt method. As the dynamic solution progresses in time, the normal components of the nodal displacements along the crack flanks are computed at each time step to monitor the opening and closing of each crack. When closure occurs at nodal pairs along a crack, the corresponding nodes are prevented from overlapping by introducing stiff dimensionless springs. These remain in place as long as the nodes stay in contact, but are removed if the nodes tend to move away from each other in a subsequent time step.

The times of propagation of the cracks are determined from concepts of linear elastic fracture mechanics. Both modes I and II stress intensity factors are computed at all time steps and the maximum tensile strain theory is used to derive the criterion for crack propagation. This theory employs the dynamic fracture toughness K_{Id} as the material parameter governing fracture and provides also the direction of crack growth at the instant of crack instability. When a crack is detected to be unstable, the direction of crack propagation is computed and the crack tip is advanced by modifying the boundary element mesh along the extended crack line. The details of this procedure have been discussed previously (Pekau and Batta,1992).

The choice of a suitable magnitude for crack extensions is important because it affects directly the computational efficiency and possibly also the predicted crack path. Based on the results of the parametric investigation reported earlier (Pekau and Batta, 1994), a piecewise extension of 10 percent of the instantaneous crack length, but limited to a maximum increment of 1.0 m, is employed.

NUMERICAL RESULTS

For the present case study the tallest monolith of the Pine Flat dam, shown in Figure 1(a), is selected in order to investigate the seismic cracking behavior of a gravity dam possessing typical geometry. The following

material properties are employed for the mass concrete of the dam: modulus of elasticity = 22400 MPa, Poisson's ratio = 0.2 and density = 2400 kg/m^3. In the absence of test values, the dynamic tensile strength of the concrete is assumed to be 3.66 MPa, which is also the value used by Vargas-Loli and Fenves (1989).

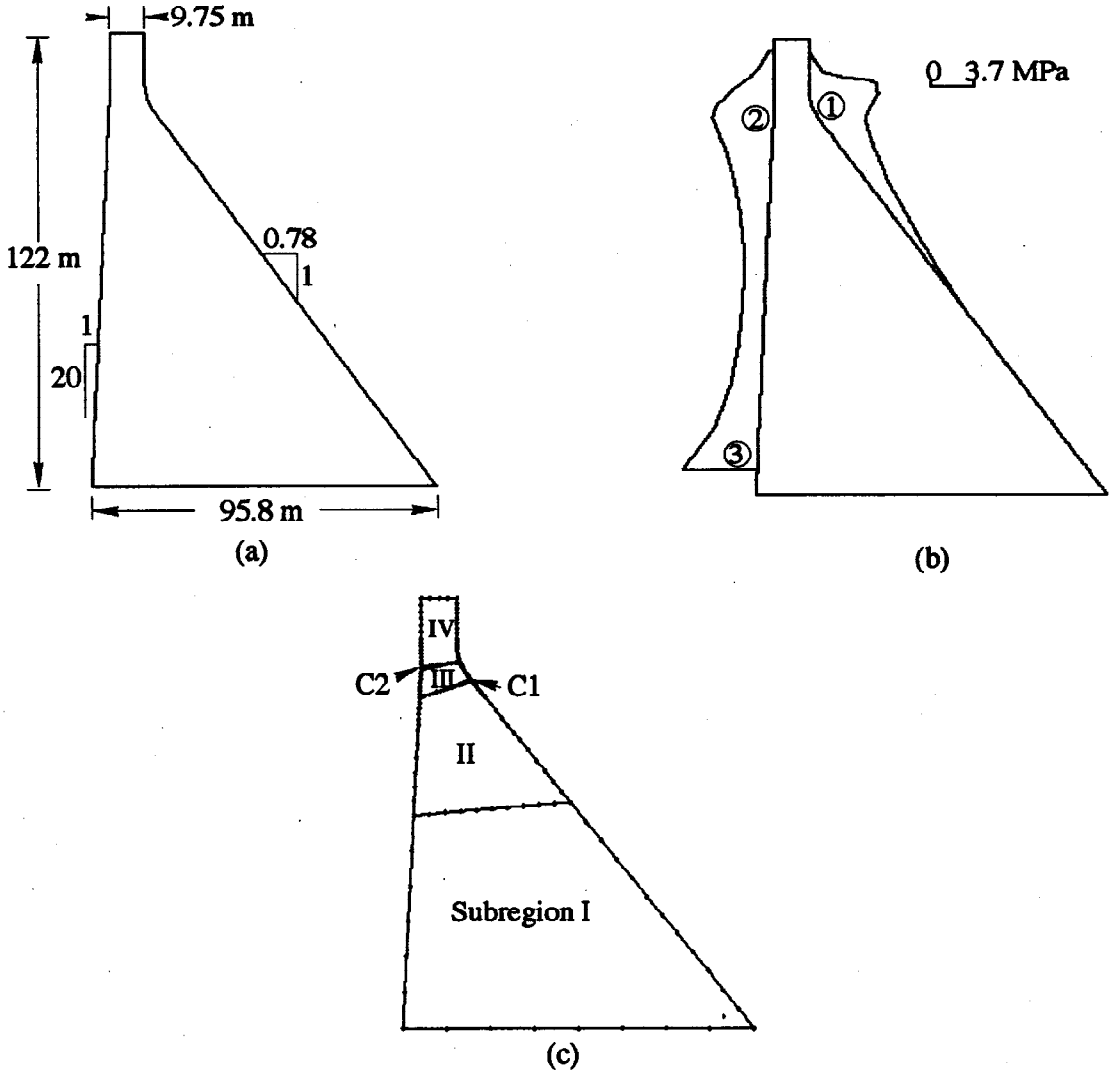

Fig. 1 Pine Flat dam: (a) geometry; (b) linear elastic tensile stress envelope; (c) boundary element discretization

Damping equal to 5 percent is assumed for the first two modes of vibration of the dam. Three different values for the dynamic fracture toughness of the concrete, namely K_{Id} = 2.0, 5.5 and 9.0 MPa.m$^{1/2}$ are employed because of the uncertainty associated with the determination of the magnitude of this parameter.

The dam-reservoir interaction is approximated using the added mass concept with the depth of water taken as 116 m (full reservoir condition). The base of the dam is considered to be fixed and water pressure effects in the cracks on the upstream face of the dam are not considered. The S69E component of the ground motion recorded at the Taft Lincoln School Tunnel during the Kern County, California, earthquake of July 21, 1952 is selected as the excitation for the fracture study. Only the horizontal component of this ground motion (PGA = 0.18g) acting in the stream-wise direction is used.

Linear Analysis and Locations of Potential Cracking

In order to identify the zones of potential cracking, a linear elastic analysis of the dam is performed for 6 sec

of the ground motion. Peak tensile stress in the dam is found, however, not to exceed the assumed tensile strength of the concrete. In order to induce cracking, the ground acceleration is amplified by a factor of 2.5 for which the corresponding envelope of principal tensile stresses on the faces of the dam is depicted in Fig. 1(b). Three potential zones of cracking can be identified, namely two in the top portion of the dam (zones 1 and 2) and one (zone 3) near the heel.

Since it has been demonstrated by Chapuis *et al.* (1985) that cracking in zone 3 is not critical, the following multiple crack propagation analysis of the dam considers two initial 1.0 m long cracks, one each in zones 1 and 2. Thus, initial cracks C1 and C2 are introduced, respectively, on the downstream and the upstream faces of the dam. Crack C1 is modelled at elevation 98 m, whereas crack C2 on the upstream face is taken at elevation 102 m. The corresponding boundary element discretization of the dam with initial cracking is shown in Fig. 1(c) and comprises 180 nodes and 117 boundary elements. Crack propagation analysis is performed employing the aforementioned (scaled) ground motion with a time step of 0.003 sec.

Results of Fracture Analysis

Results for the fracture response of the dam are presented in Fig. 2. As shown by the final profiles for the two initial cracks depicted in Fig. 2(a), complete separation of the crest block is predicted with cracks C1 and C2 propagated to merge within the body of the dam. It is worth noting that the computed final profile of crack C1 is almost perpendicular to the downstream face and matches the profile of a similar crack obtained in the laboratory rupture test of the dam by Donolon and Hall (1989).

The influence of the presence of a long crack on the path followed by a crack on the opposite face of the dam is evident in Fig. 2(a). Upstream crack C2, which propagates later [Fig. 2(b)], begins to extend horizontally but reorients itself towards the tip of already propagated crack C1 during its subsequent growth. This change in direction is the consequence of a change in the orientation of the stress field ahead of the tip of crack C2, caused by the increase in shear stress in the intact concrete between the two crack tips. The downward growth of crack C2, however, also brings the tip of this crack sufficiently close to crack C1 to result in complete rupture of the dam cross-section.

The corresponding time histories of crack lengths for C1 and C2 are shown in Fig. 2(b), where it is seen that the propagation processes for the two cracks take place almost instantaneously. The propagation of

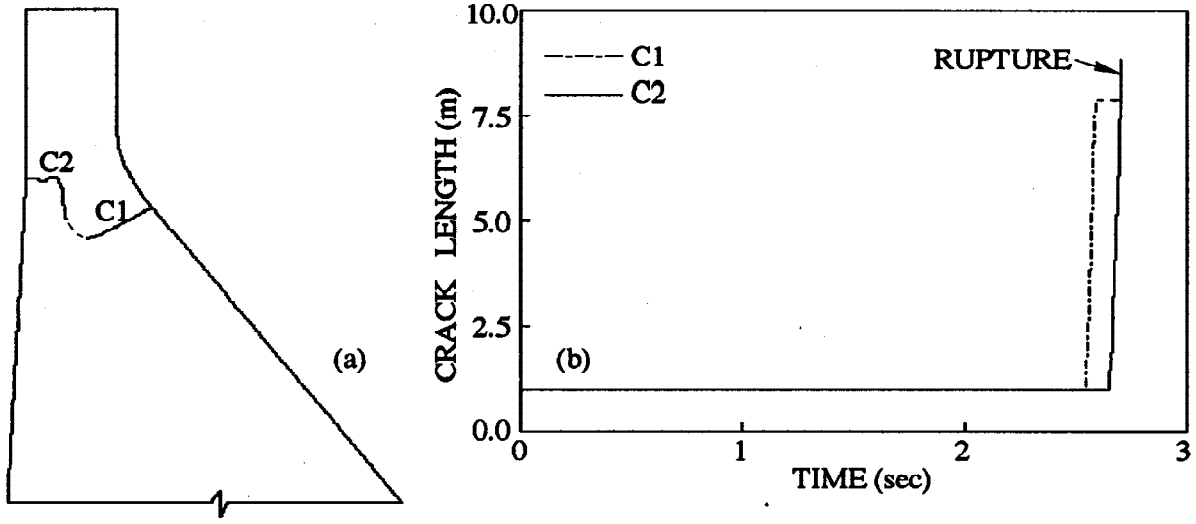

Fig. 2 Fracture process for K_{Id} =2.0 MPa.m$^{1/2}$: (a) final cracking profile; (b) time-histories of crack lengths

downstream crack C1, which begins to grow first, is completed in a single stage during only 0.04 sec, while the corresponding elapsed time for the propagation of C2 is 0.05 sec.

The time history of horizontal displacement of the dam crest is presented in Fig. 3(a), where the corresponding data from the linear elastic analysis of the uncracked dam is also depicted. Although the fracture process can be seen to influence the crest displacement, it is evident that the deviation in the two time histories is not significant over most of the time-history. However, with the dam cross-section nearly ruptured, larger magnitude of the crest displacement is obtained, with a maximum difference in the peak crest

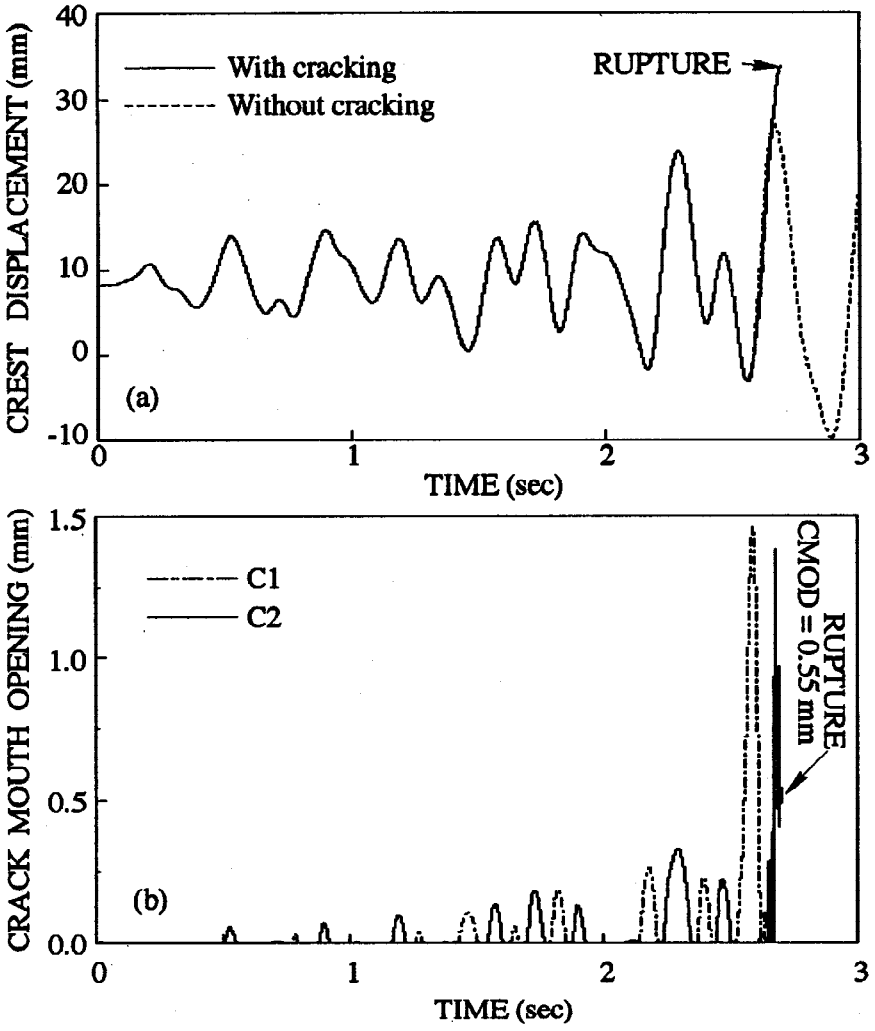

Fig. 3 Response time histories: (a) crest displacement; (b) crack mouth openings

displacement of approximately 7 mm at rupture. Noting that the positive displacement indicates movement toward downstream, it is also observed in Fig. 3(a) that the crest is displaced in the upstream direction when the downstream crack C1 begins to propagate, and that crack C2 becomes unstable in the same cycle when the crest movement reverses. The corresponding maximum openings of the two crack mouths [Fig. 3(b)] are, however, not proportional to the displacement magnitudes of the crest.

Examining the crack mouth opening data in Fig. 3(b), it is evident that the two cracks open and close alternately, with comparable magnitudes for the entire time history until rupture. The mouth opening at initiation of propagation of downstream crack C1 is 0.45 mm, following which the crack continues to open to

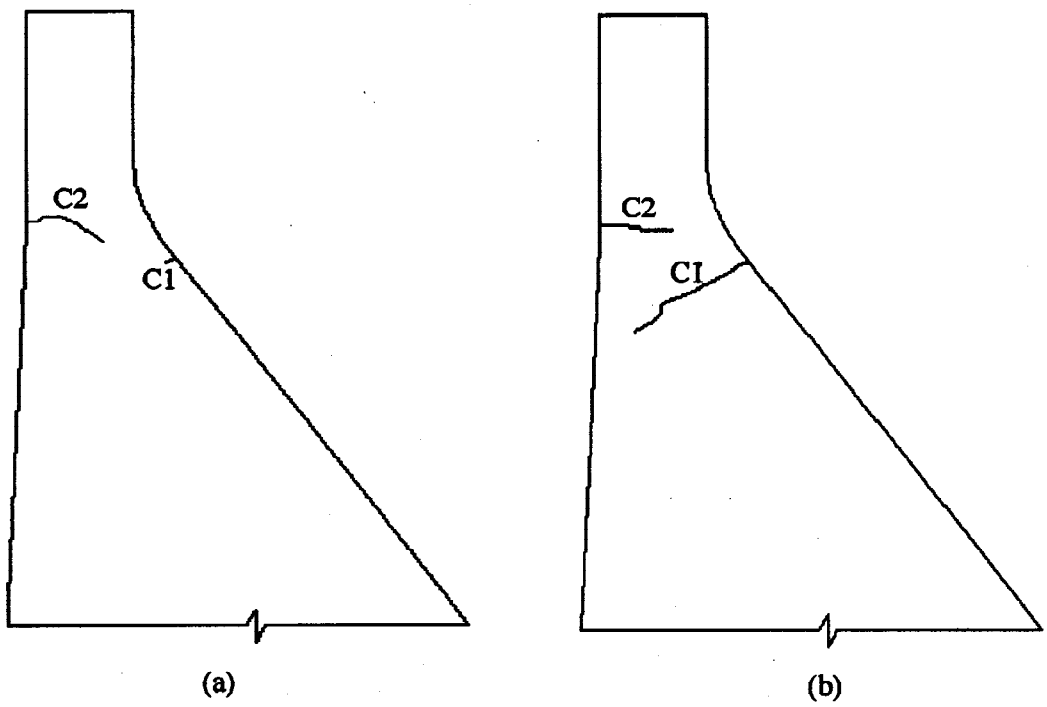

Fig. 4 Final cracking profiles for higher magnitudes of dynamic fracture toughness: (a) K_{Id} = 5.5 MPa.m$^{1/2}$; (b) K_{Id} = 9.0 MPa.m$^{1/2}$

a maximum of 1.46 mm while also extending in length. Similarly for crack C2, comparable magnitude of opening of 0.525 mm at instability is predicted, with a maximum opening of this crack during the rupture phase of 1.38 mm. Furthermore, the first major opening for each crack coincides with crack instability and results in complete rupture which, as noted above, occurs in a single reversal of the crest movement. It is interesting to note that similar behavior was reported previously (Batta and Pekau, 1996) for the Koyna dam when undergoing single crack propagation.

Effect Of Higher Concrete Fracture Toughness

Results for the multiple crack propagation analysis with two higher values of the fracture toughness are presented in Fig. 4, where the final profiles of cracks C1 and C2 for K_{Id} = 5.5 and 9.0 MPa.m$^{1/2}$ are shown. Comparing these crack profiles with those for K_{Id} = 2.0 MPa.m$^{1/2}$ of Fig. 2(a), it is evident that final cracking in the dam is significantly different for the three values of the concrete fracture toughness. For K_{Id} = 9.0 MPa.m$^{1/2}$, the two cracks propagate deep into the body of the dam, but neither do they penetrate the cross-section independently nor merge with each other to result in complete rupture. On the other hand, for K_{Id} = 5.5 MPa.m$^{1/2}$, although propagating crack C2 appears in Fig. 4(a) to be heading toward downstream crack C1, the fracture analysis could not be completed because the tip of this crack approaches to intersect the subdomain boundary emanating from crack C1. Further rediscretization with the current boundary element mesh could not therefore be performed.

From other crack propagation data (not shown) for the two higher magnitudes of the fracture toughness, it is observed that the initiation of crack extension is delayed as the fracture toughness is increased. As a result, larger envelope values of tensile stresses are predicted in the dam for the higher magnitudes of concrete toughness. For example, it can be seen from Fig. 5 that the envelope tensile stresses computed on the two faces of the dam for K_{Id} = 9.0 MPa.m$^{1/2}$ exceed the tensile strength of concrete over most of the top portion of the dam. Distributed surface cracking is therefore likely to occur if the fracture toughness is sufficiently high.

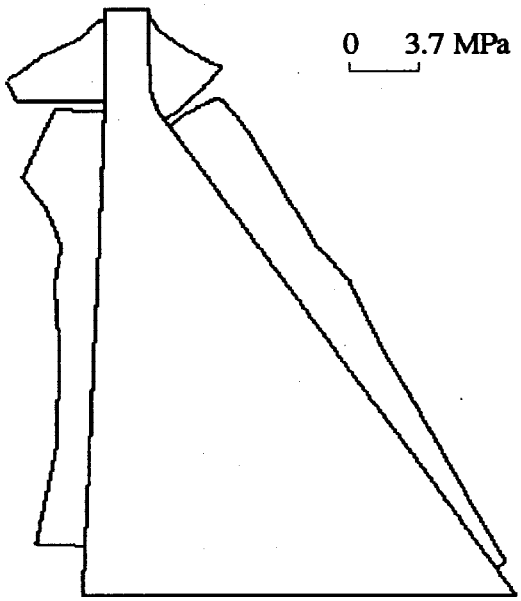

Fig. 5 Envelope of principal tensile stresses for K_{Id} = 9.0 MPa.m$^{1/2}$

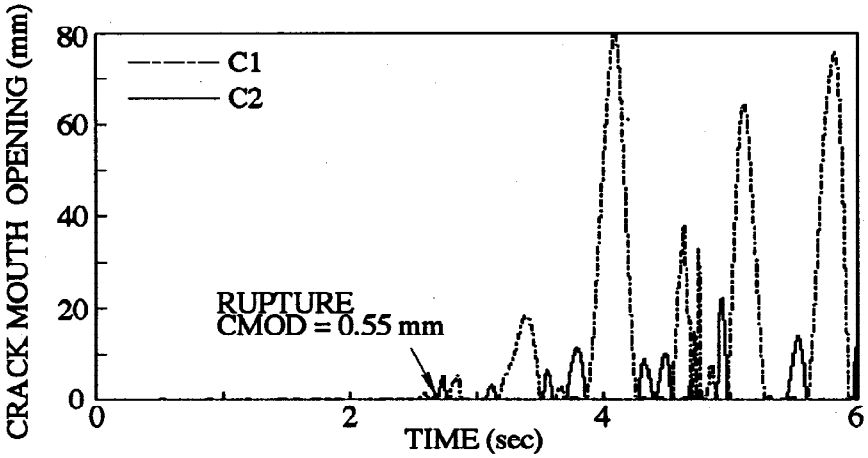

Fig. 6 Post-rupture behavior for K_{Id} = 2.0 MPa.m$^{1/2}$

Post-cracking Behavior

Since hydrodynamic uplift pressure in upstream cracks is of concern to dam engineers and because this pressure can also be expected to build up further during the remaining time history of the earthquake excitation after rupture, the opening data for crack C2 on the upstream face of the dam is obtained by performing approximate post-rupture analysis. The analysis is performed only for K_{Id} = 2.0 MPa.m$^{1/2}$, for which complete rupture was predicted. Hypotheses involved in such continuation of the time history analysis beyond the fracture phase have been discussed elsewhere (Batta and Pekau, 1996) for the case of Koyna dam.

The resulting time history of crack mouth opening for the full 6 sec of ground excitation is presented in Fig. 6. Clearly, the magnitude of opening of upstream crack C2 is much larger during the post-rupture phase compared to that at rupture. Since complete penetration of the dam cross-section occurs at an early stage of the earthquake excitation, the remaining strong ground motion results in significant movement of the dam crest and consequent large crack openings. Although downstream crack C1 experiences very large openings (maximum opening = 80 mm), the more relevant upstream crack C2 also undergoes a number of opening

phases with significant magnitudes. The durations of these openings are, however, small and the almost completely separated top part of the dam continues to exhibit stable response. The maximum opening of upstream crack C2 in the post-rupture phase is 22.3 mm compared to 1.38 mm during the rupture phase. Furthermore, magnitudes greater than 10 mm can also be noticed in four other cycles during the post-rupture phase, although the opening durations are all of the order of 0.1 sec.

CONCLUDING REMARKS

From the results presented herein it is observed that seismic cracking of the Pine Flat dam is likely to be concentrated near the base of the crest block, with the final cracking pattern involving complete rupture of the dam cross-section. Moreover, due to the almost instantaneous propagation of the cracks, the rupture process itself is short. Increasing magnitudes of fracture toughness of the concrete influence the final cracking pattern in the dam and, for sufficiently high values, cracking is more distributed due to the delay in the propagation of already existing cracks. Furthermore, openings of the upstream crack are greatly increased during the post-rupture phase compared to the pre-rupture and rupture phases, making possible that significant dynamic uplift pressure will develop in such cracks during the post-rupture response. The stability of the separated upper portion of the dam will therefore be influenced by the presence of the increased uplift pressure during post-rupture seismic response. Finally, the data from the fracture analysis of the Pine Flat dam presented in this paper has served also to confirm that the observations and conclusions arising out of the corresponding Koyna dam investigation presented earlier by the authors (Batta and Pekau, 1996) can be viewed as generally applicable to concrete gravity dams.

REFERENCES

Ayari, M. L. and V .E. Saouma (1990). A fracture mechanics based seismic analysis of concrete gravity dams using discrete cracks. *Engng. Fract. Mech.*, 35 (1/2/3), 587-598.

Batta, V. and O. A. Pekau (1996) . Application of boundary element method for multiple seismic cracking in concrete gravity dams. *Earthquake Eng. Struct. Dyn.*, to appear.

Bhattacharjee, S. S. and P. Léger (1993). Seismic cracking and energy dissipation in concrete gravity dams. *Earthquake Eng. Struc. Dyn.*, 22, 991-1007.

Chapuis, J., B. Rebora, and Th. Zimmermann. (1985). Numerical approach of crack propagation analysis in gravity dams during earthquakes. *ICOLD* , Lausanne, 57(26), 451-473.

Donolon, W. P. and J. F. Hall (1991). Shaking table study of concrete gravity dam monoliths. *Earthquake Eng. Struct. Dyn.*, 20, 769-786.

El-Aidi, B. and J. F. Hall (1989a). Non-linear earthquake response of concrete gravity dams part 1: modelling. *Earthquake Eng. Struc. Dyn.* , 18, 837-851.

El-Aidi, B. and J. F. Hall (1989b). Non-linear earthquake response of concrete gravity dams part 2: behavior- *Earthquake Eng. Struc. Dyn* ., 18, 853-865.

Pekau, O. A., C. Zhang, and L. Feng (1991). Seismic fracture analysis of concrete gravity dams. *Earthquake Eng. Struct. Dyn.*, 20, 335-354.

Pekau, O. A. and V. Batta (1992). Seismic cracking of concrete structures using boundary element method. *Int. J. Num. Meth. Engng.*, 35, 1547-1564.

Pekau, O. A. and V. Batta (1994). Seismic Cracking Analysis of Concrete Gravity Dams. *Dam Engineering*, 5(1), 5-29.

Vargas-Loli, L. M. and G. L. Fenves (1989). Effects of concrete cracking on the earthquake response of gravity dams. *Earthquake Eng. Struct. Dyn.* , 18, 575-592.